A *TARBP2* mutation in human cancer impairs microRNA processing and DICER1 function

Sonia A Melo[1], Santiago Ropero[1], Catia Moutinho[1], Lauri A Aaltonen[2], Hiroyuki Yamamoto[3], George A Calin[4], Simona Rossi[4], Agustin F Fernandez[1], Fatima Carneiro[5], Carla Oliveira[5], Bibiana Ferreira[1], Chang-Gong Liu[4], Alberto Villanueva[6], Gabriel Capella[6], Simo Schwartz Jr[7], Ramin Shiekhattar[8,9] & Manel Esteller[1,9,10]

microRNAs (miRNAs) are small noncoding RNAs that regulate gene expression by targeting messenger RNA (mRNA) transcripts. Recently, a miRNA expression profile of human tumors has been characterized by an overall miRNA downregulation[1–3]. Explanations for this observation include a failure of miRNA post-transcriptional regulation[4], transcriptional silencing associated with hypermethylation of CpG island promoters[5–7] and miRNA transcriptional repression by oncogenic factors[8]. Another possibility is that the enzymes and cofactors involved in miRNA processing pathways may themselves be targets of genetic disruption, further enhancing cellular transformation[9]. However, no loss-of-function genetic alterations in the genes encoding these proteins have been reported. Here we have identified truncating mutations in *TARBP2* (TAR RNA-binding protein 2), encoding an integral component of a DICER1-containing complex[10,11], in sporadic and hereditary carcinomas with microsatellite instability[12–14]. The presence of *TARBP2* frameshift mutations causes diminished TRBP protein expression and a defect in the processing of miRNAs. The reintroduction of TRBP in the deficient cells restores the efficient production of miRNAs and inhibits tumor growth. Most important, the TRBP impairment is associated with a destabilization of the DICER1 protein. These results provide, for a subset of human tumors, an explanation for the observed defects in the expression of mature miRNAs.

In order to explore the presence of inactivating mutations in the so-called 'miRNA processing machinery genes' it is useful to consider tumors that show microsatellite instability, both in the context of hereditary nonpolyposis colon cancer (HNPCC) associated with germline mutations in the mismatch repair genes[14] and in sporadic cancers associated with hMLH1 inactivation by promoter CpG island methylation[12,13]. Tumors with microsatellite instability progress along a genetic pathway with a high rate of insertion and deletion mutations in mononucleotide repeats, which often results in the generation of premature stop codons. Illustrative target genes include the growth-control gene *TGFBR2* (ref. 15) and the proapoptotic gene *BAX*[16].

We first screened six colorectal (Co115, RKO, SW48, LoVo, HCT-15 and HCT-116), four endometrial (SKUT-1, SKUT-1B, AN3CA and HEC1B) and two gastric (SNU-1 and SNU-638) cancer cell lines with microsatellite instability for the presence of mutations in all the exonic mononucleotide repeats present in the coding sequences of eight established members of the miRNA processing machinery: the RNase III family of double-stranded RNases (DICER1 and DROSHA), RNA-binding proteins that act as catalytic partners (DGCR8, TRBP and PACT) and Argonaute members (AGO1, AGO2 and AGO4). The location of the corresponding repeats and the PCR primers used are shown in the **Supplementary Table 1** online. We detected only wild-type sequences for all the genes described, with the single notable exception of *TARBP2* (**Fig. 1a**). We found two frameshift mutations in *TARBP2*: the deletion of a C in a $(C)_5$ coding microsatellite repeat of exon 5 in the colorectal cancer cell line Co115 and the insertion of a C in a $(C)_7$ coding microsatellite repeat of exon 5 in the endometrial cancer cell line SKUT-1B (**Fig. 1a**). The *TARBP2* mutations were present in 29 of 41 (71%) and 17 of 31 (55%) single-clone sequences obtained from genomic DNA for Co115 and SKUT-1B, respectively. The same proportion of mutant alleles was found when we used cDNA as starting material; thus, these are heterozygous mutations. The two alleles of *TARBP2* were retained in both cell lines according to the FISH analysis (**Supplementary Fig. 1** online). We analyzed TRBP
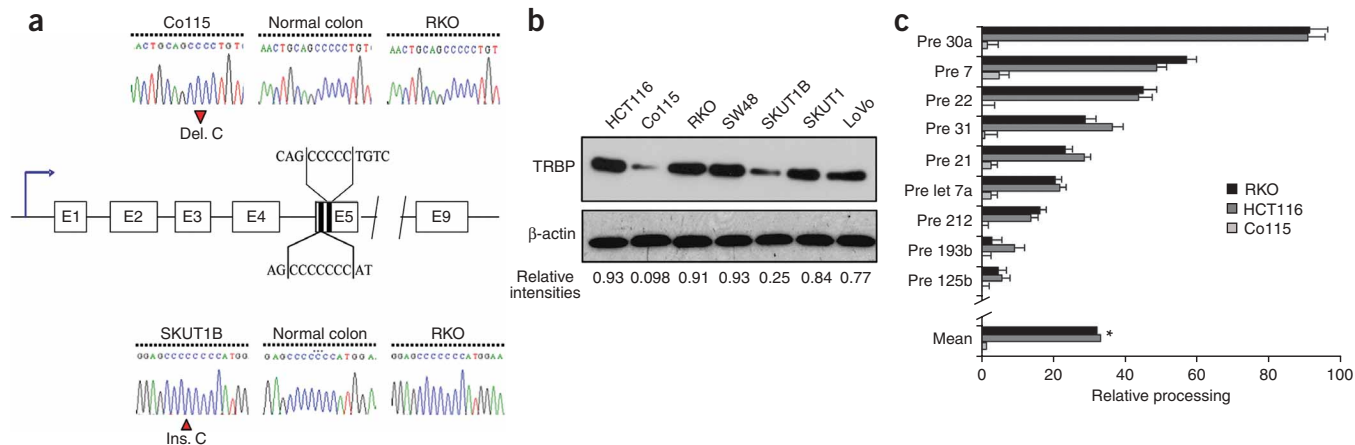
Figure 1 A mutant *TARBP2* in human cancer. (**a**) Schematic representation of the *TARBP2* gene, with the location of the (C)₇ and (C)₅ repeats, and electropherograms of *TARBP2* wild-type (normal colon, RKO, HCT116 and SKUT1) and mutant (Co115 and SKUT1B) cells. (**b**) TRBP protein expression analyzed by protein blot was very low and diminished in the mutant Co115 and SKUT1B cells, respectively, but not in the other colon and endometrial cancer cell lines with a wild-type sequence. Quantitation values using densitometric software are shown. (**c**) Relative processing of endogenous precursor miRNAs in *TARBP2* mutant (Co115) cell line was significantly reduced compared with *TARBP2* wild-type (RKO and HCT116) cell lines (the results shown are the average of three independent studies *$P < 0.001$). Relative processing was defined as the ratio of mature to precursor miRNA. Error bars, s.e.m.

protein expression in Co115 and SKUT-1B cell lines and found very low and diminished expression, respectively (**Fig. 1b**). We did not observe any evidence of *TARBP2* mutations in colorectal (SW480, SW620 and COLO205) and endometrial (KLE) cancer cell lines that lacked microsatellite instability.

Once the presence of inactivating mutations of *TARBP2* in cancer cells had been confirmed, it became very important to establish whether they affect the processing efficiency of pre-miRNAs. We first assessed the processing efficiency of pre-miRNAs in *TARBP2* mutant colorectal cancer cells (Co115) in comparison with *TARBP2* wild-type colorectal cancer cells (RKO and HCT116)[17]. We found that TRBP-deficient cells featured a mean 90% reduction in the efficiency of endogenous processing miRNAs relative to TRBP-proficient cells

(**Fig. 1c**). To strengthen the evidence of a link between *TARBP2* mutations and the impaired miRNA phenotype observed, we reconstituted TRBP function in TRBP-deficient cancer cells (Co115) (**Fig. 2** and **Supplementary Fig. 1**). Transfection of wild-type *TARBP2* in Co115 cells (**Fig. 2a**) restored the pre-miRNA processing capacity for both the endogenous pre-miRNAs (**Fig. 2b,c**) and for the synthetic precursor molecules that we had introduced (**Fig. 2d**). Pri-miRNA concentrations did not change upon *TARBP2* transfection (**Supplementary Fig. 1**). Transfection of the mutant form of *TARBP2* (C deletion of the (C)₅ coding repeat in exon 5) in Co115 cells (**Fig. 2a**) was unable to restore pre-miRNA processing capacity (**Fig. 2b,d**). We then used a microarray platform[18] to study the global miRNA expression profile of Co115 cells upon transfection of wild-type *TARBP2*. We

Figure 2 Transfection of wild-type *TARBP2* rescues pre-miRNA processing capacity. (**a**) TRBP protein expression was restored after transfecting wild-type *TARBP2* in Co115 cell line. Stable clones were selected treating cells with puromycin (left). As a control, the truncated form of *TARBP2*, due to the mutation in the (C)₅ repeat, was also transfected in a pCMV-Tag4b vector and tested using an antibody against Flag. Stable clones were selected using G418. (**b**) Co115 cell line transfected with wild-type *TARBP2* presented a 3.6-fold increase in the capacity of processing the existing precursor miRNAs compared with cells transfected with empty vector. No changes were observed in cells transfected with the *TARBP2* truncated form in comparison to cells transfected with empty vector. *$P < 0.001$. (**c**) RNA blot analysis confirmed a defect in the generation of mature miRNAs in *TARBP2* mutant Co115 cells that was rescued by transfection of wild-type *TARBP2*. (**d**) Synthetic precursor molecules were transiently transfected in Co115 cells that stably expressed *TARBP2* wild-type and truncated form, versus cell lines transfected with empty vector. Only in Co115 cells transfected with wild-type *TARBP2* did we observe an increase in the capacity to process the transfected precursor molecules. **$P < 0.005$. (**e**) The use of a miRNA microarray platform showed an increase in the number of overexpressed mature miRNAs in the Co115 *TARBP2*-transfected cells, whereas transfection of the *TARBP2* mutant form did not cause any miRNA overexpression. Error bars, s.e.m.
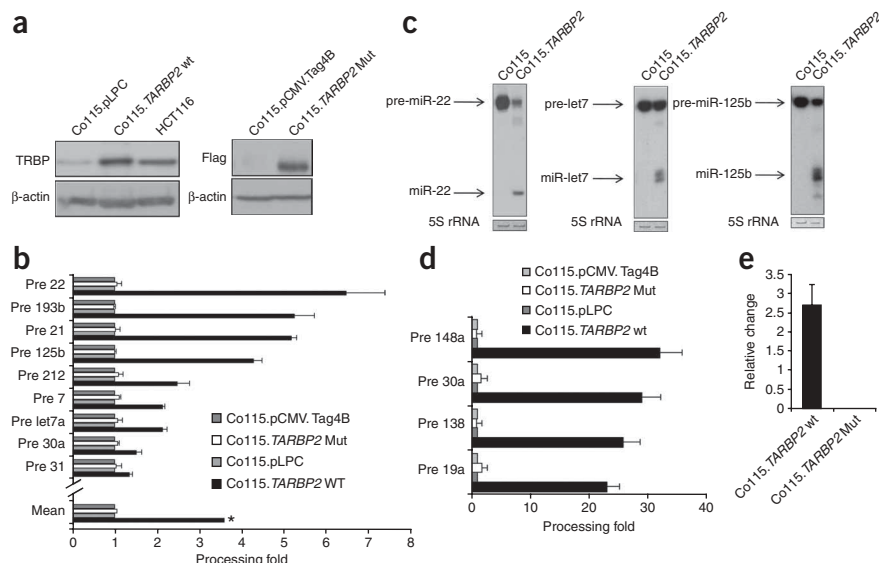
Figure 3 *TARBP2* mutation impairs DICER1 protein. (**a**) DICER1 protein expression analyzed by protein blot was very low and diminished in the *TARBP2* mutant Co115 and SKUT1B cell lines, respectively, but present in cancer cell lines with wild-type *TARBP2* sequences. (**b**) DICER1 protein concentrations analyzed by protein blot were restored after transfection of wild-type *TARBP2* in Co115 cell line. The transfection with the truncated form of *TARBP2* did not restore DICER1 concentrations. (**c**) DICER1 protein concentrations were restored after transfecting *DICER1* in Co115 cells. *DICER1* transfection was unable to restore TRBP expression because these cells harbor the frameshift mutation in the *TARBP2* gene. Stable clones were selected by treating cells with G418. (**d**) Co115 cells transfected with *DICER1* show a mean 3.2-fold induction on the processing efficiency of precursor miRNAs in comparison cells transfected with empty vector. (**e**) Co115 cells transfected with *DICER1* show a higher rate of processing synthetic precursor miRNA molecules in comparison to cells transfected with empty vector. Error bars, s.e.m.
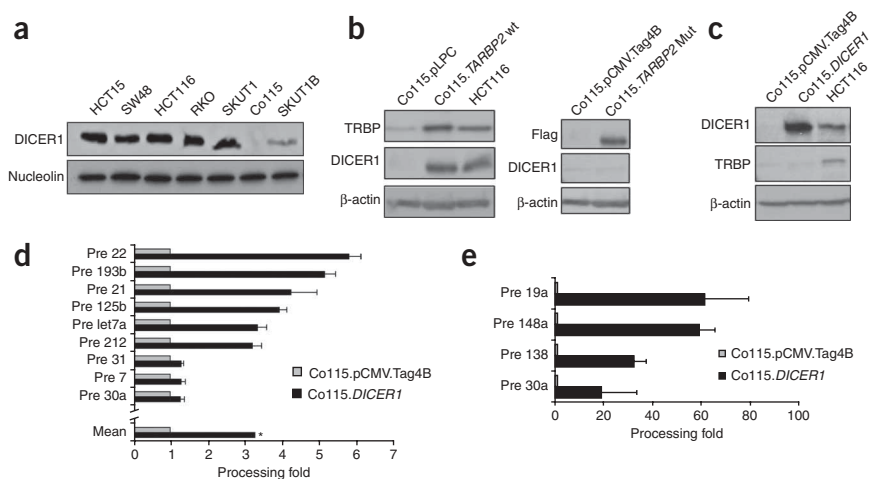
observed a 2.7-fold increase in the number of overexpressed mature miRNAs in the *TARBP2*-transfected cells in comparison to empty vector transfected cells (**Fig. 2e**), whereas transfection of the *TARBP2* mutant form did not change the miRNA expression profile (**Fig. 2e**). An annotated heat map of the miRNA microarray expression data and the validated results of 33 miRNAs by qRT-PCR are shown in **Supplementary Figure 2** online. Most of the miRNAs upregulated by *TARBP2* transfection in mutant cells have potential tumor suppressor capacities, such as let-7f[19], miR-205[20], miR-26a[21], miR-125a[22] and miR-125b[22]. Indeed, transfection of these miRNAs in Co115 increased the doubling time of these cells (**Supplementary Fig. 3** online). The reintroduction of TRBP in the deficient cells was also associated with the downregulation of the oncoproteins targeted by these miRNAs, such as ERBB2 and EZH2 (refs. 21,22 and **Supplementary Fig. 2**). In contrast, the downregulation of TRBP by RNA interference in *TARBP2* wild-type cells (RKO) caused an impairment of pre-miRNA processing (**Supplementary Fig. 1**).

TRBP is an integral component of a DICER1-containing complex[10,11]; it interacts directly with the DICER1 protein[10,11] and is required for the stabilization of the DICER1 protein[10]. This prompted us to consider how the presence of *TARBP2*-inactivating mutations affect DICER1 activity. When we analyzed the expression of the DICER1 protein in *TARBP2* wild-type colorectal cancer cell lines and the *TARBP2* mutant Co115 cells, this latter cell line was the only one in which DICER1 protein expression was extremely low (**Fig. 3a**). For the endometrial cancer cell lines, mutant *TARBP2* SKUT-1B cells also presented diminished DICER1 protein concentrations compared to wild-type SKUT-1 cells (**Fig. 3a**). We did not observe *DICER1* mutation, promoter CpG island methylation, genomic loss or increased ubiquitin-protein degradation (**Supplementary Fig. 4** online). When we reconstituted TRBP expression in Co115 cells by transfection of a wild-type *TARBP2* construct, the protein expression of DICER1 was restored (**Fig. 3b**). The transfected mutant form of *TARBP2* was unable to rescue DICER1 protein expression (**Fig. 3b**). Protein translation inhibition by cycloheximide in Co115 cells was unable to show DICER1 stabilization, but it was observed upon *TARBP2* transfection, as it also occurred in wild-type *TARBP2* cancer cells (**Supplementary Fig. 4**). These results are evidence that the loss of TRBP results in the destabilization of the DICER1 protein[10] and underpin the absence of a functional DICER1–TRBP complex in Co115 cells.

Having demonstrated that the *TARBP2* mutant cells also had a secondary associated defect in DICER1, we reconstituted DICER1 activity (**Fig. 3c**). The Co115 *DICER1*-transfected cells were not able to restore TRBP protein concentrations because the *TARBP2* mutation was present (**Fig. 3c**); however, they relatively increased the efficacy of miRNA processing in the endogenous pre-miRNAs (**Fig. 3d**) and in those introduced exogenously (**Fig. 3e**). The cotransfection of *TARBP2* and *DICER1* in Co115 *TARBP2* mutant cells caused a slightly higher miRNA processing fold than for each single gene (**Supplementary Fig. 5** online). In contrast, the downregulation of *DICER1* by RNA interference in cells with wild-type *TARBP2* (RKO) was associated with impaired pre-miRNA processing (**Supplementary Fig. 6** online).

Most notably from the tumor biology standpoint, the ectopic expression of TRBP in the deficient cells induced tumor suppressor–like features (**Fig. 4**). Upon restoration of TRBP expression in Co115 TRBP-deficient colorectal cancer cells, the cells proved less viable in the MTT assay (**Fig. 4a**) and markedly reduced percentage colony formation density (**Fig. 4b**). Transfection of the mutant form of *TARBP2* in Co115 cells was unable to reduce cell viability (**Fig. 4a**) and had no impact on the colony formation assay (**Fig. 4b**). Overexpression of TRBP in the wild-type *TARBP2* colorectal cancer cell line RKO was unable to reduce cell viability (**Supplementary Fig. 6**). We next tested the ability of *TARBP2*-transfected Co115 cells to form tumors in nude mice (**Fig. 4c**). Co115 TRBP-deficient cells transfected with the empty vector or the mutant gene formed tumors rapidly, but cells transfected with the wild-type *TARBP2* had much lower tumorigenicity (**Fig. 4c**). In contrast, the downregulation of *TARBP2* by short hairpin RNA in cells with wild-type *TARBP2* (RKO and HCT-116) was associated with increased viability and clonogenicity (**Supplementary Fig. 6**).

Notably, the reintroduction of *DICER1* in Co115 *TARBP2* mutant cells also showed tumor-suppressor properties: the cells were less viable in the MTT assay (**Fig. 4d**), they had a lower percentage colony formation density (**Fig. 4e**) and their ability to form tumors in nude mice was lower (**Fig. 4f**). The cotransfection of *TARBP2* and *DICER1* together inhibited colony formation and the development of tumors in mice to a slightly greater extent (**Supplementary Fig. 5**). These data showing how both the loss of *TARBP2* and/or *DICER1* compromises precursor miRNA processing and the potential tumor-suppressor features of both genes are consistent with the recently described
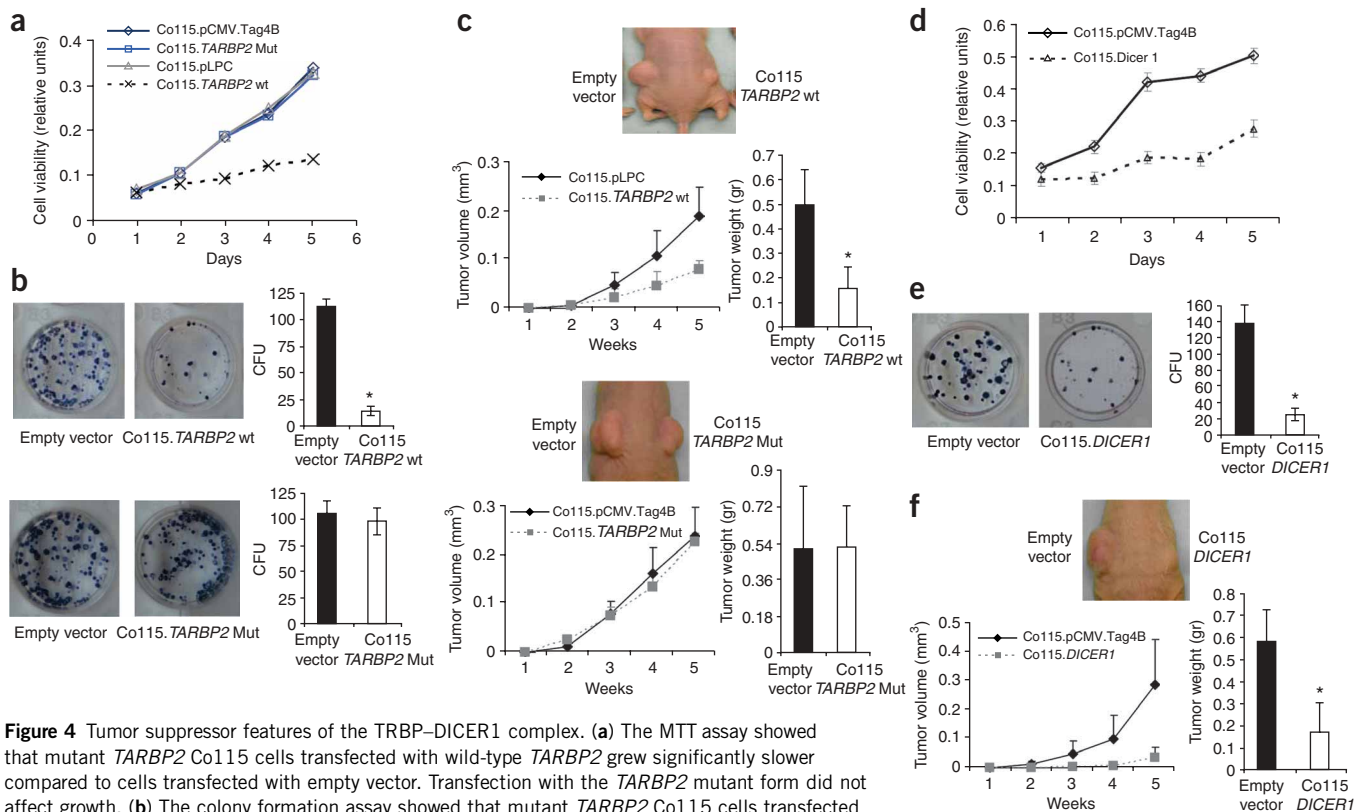
Figure 4 Tumor suppressor features of the TRBP–DICER1 complex. (**a**) The MTT assay showed that mutant *TARBP2* Co115 cells transfected with wild-type *TARBP2* grew significantly slower compared to cells transfected with empty vector. Transfection with the *TARBP2* mutant form did not affect growth. (**b**) The colony formation assay showed that mutant *TARBP2* Co115 cells transfected with wild-type *TARBP2* formed significantly less colonies in comparison to cells transfected with empty vector (*$P < 0.001$). Transfection with the *TARBP2* mutant form did not affect colony formation. (**c**) Effect of *TARBP2* transfection on the growth of Co115 cells in nude mice. Tumor volume was monitored over time, and the tumor was excised and weighed at 30 d. Note the large tumor on the left flank, corresponding to cells transfected with empty vector, and the reduced tumor on the opposite flank, corresponding to cells transfected with wild-type *TARBP2*. Transfection of mutant *TARBP2* did not affect tumor growth. (**d–f**) Co115 cells transfected with *DICER1* also showed reduced cell viability (**d**), diminished colony formation (**e**) and tumor growth inhibition in nude mice (**f**) in comparison to cells transfected with empty vector.

enhancement of cellular transformation and tumorigenesis upon depletion of *DICER1* in human cells[9] and in a conditional deletion of *DICER1* in a mice model[9]. Most important, reduced *DICER1* expression has been observed in lung tumors associated with poor prognosis[23]. Thus, our data underline the proposed role of different components of the miRNA processing machinery, and a subgroup of miRNAs, as tumor suppressor genes[19].

Finally, we sought to measure the frequency of the described *TARBP2* disruption in human primary tumors. We assessed the *TARBP2* mutational status of 282 human primary malignancies with microsatellite instability, including colorectal tumors from individuals with HNPCC ($n = 30$) and sporadic colorectal ($n = 209$) and gastric ($n = 43$) malignancies (**Table 1**). We found that *TARBP2* frameshift mutations were present in 26% (72 of 282) of the primary tumors analyzed. The deletion of a C in the $(C)_5$ coding microsatellite repeat of exon 5 was noted in 63 cases and there was an insertion of a C in a $(C)_7$ coding microsatellite repeat of exon 5 in the remaining nine cases. No single tumor featured both mutations, which highlights the functional relevance of each mutational event. The presence of *TARBP2* wild-type sequences suggested that the mutations were heterozygous. The described *TARBP2* mutations were not present in primary colorectal tumors without microsatellite instability (0/50), normal colorectal mucosa (0/50) or in normal lymphocytes from healthy donors (0/80) (**Table 1**). *TARBP2* mutations were also absent in lymphocytes from individuals with HNPCC (0/12), in whom the corresponding colon tumors had *TARBP2* mutations (**Table 1**). For 20

cases of microdissected primary sporadic colon tumors with microsatellite instability, and 10 corresponding normal colorectal mucosa, we conducted a TRBP protein blot expression analysis (**Supplementary Fig. 7** online). In all cases with wild-type *TARBP2*, 10 primary tumors and all normal mucosa samples, TRBP protein was strongly expressed. In contrast, the 10 *TARBP2* mutant tumors demonstrated diminished expression of the TRBP protein (**Supplementary Fig. 7**).

In summary, we have demonstrated the presence of inactivating mutations in the gene encoding the RNA-binding protein TRBP, an essential functional partner of DICER1, in human cancer cell lines and

Table 1 Frequency of *TARBP2* mutations in cancer cell lines, primary tumors and normal tissues

Sample type	Cell lines	Tissue samples
Colon tumors from HNPCC	–	13/30 (43.3%)
Sporadic colon tumors (MSI+)	1/6 (16.7%)	53/209 (25.4%)
Sporadic gastric tumors (MSI+)	–	6/43 (14%)
Sporadic endometrial tumors (MSI+)	1/4 (25%)	–
Sporadic colon tumors (MSI–)	0/4	0/50
Normal colon	–	0/50
Normal lymphocytes from healthy donors	–	0/80
Lymphocytes from subjects with HNPCC	–	0/12

HNPCC, hereditary nonpolyposis colon cancer; MSI+, tumors with microsatellite instability; MSI–, tumors without microsatellite instability.

primary tumors with microsatellite instability that impairs miRNA processing and enhances cellular transformation. The loss of TRBP also leads to a secondary defect in DICER1 activity. These findings are evidence of the role of loss of function events in the regulation of miRNA processing machinery during tumorigenesis. Because the restoration of efficient miRNA production can block cancer cell growth, these findings are potentially relevant to the development of new therapeutic strategies for the treatment of cancer.

METHODS

Cell lines and primary tumor samples. Human colorectal and endometrial cancer cell lines were obtained from the American Type Culture Collection. Human gastric cancer cell lines and Co115 were provided by M. Toyota (First Department of Internal Medicine, Sapporo Medical University) and R. Hamelin (Institut National de la Santé et de la Recherche Médicale), respectively. The cancer cell lines were grown and maintained in 10% FBS in RPMI medium 1640 at 37 °C in a humidified atmosphere of 5% CO_2. We obtained DNA samples from primary tumors ($n = 282$) at the time of the clinically indicated surgical procedures.

Mutation analysis. Genomic DNA from cell lines and primary tumors and cDNA from the cell lines were amplified by PCR. PCR products and recombinant plasmids from single clones of every sample were sequenced in an automated ABI Prism 3700 sequencer. The genes studied, their genomic locations and the primers used are described in **Supplementary Table 1.**

FISH analysis. FISH was done by standard methods. We used the UCSC genome browser to select for the *TARBP2* gene the two BAC clones spanning the 12q13 region: RP11-793H13 and RP11-101H10, and for *DICER1* gene the BAC clone covering the 14q32 region: RP11-1143O10. The BACs were obtained from the Children's Hospital Oakland Research Institute in Oakland, USA. We used commercial centromeric probes for chromosomes 12 and 14 (Vysis) as control.

Analysis of *TARBP2* and *DICER1* CpG island promoter methylation. DNA samples were treated with sodium bisulfite and primers spanning the CpG island of the *TARBP2* and *DICER1* promoters were used for bisulfite genomic sequencing. Primer sequences and PCR conditions are available upon request. We analyzed ten clones per sample.

Protein blotting. For protein blotting of TRBP and DICER1 expression, total protein extracts were immunoprobed with antibodies to TRBP (monoclonal ABNOVA 1:1,000) and DICER1 (1:500, Santa Cruz H212). We used an antibody against β-actin (1:5000; Sigma, St. Louis, MO) or nucleolin (1:1000; Santa Cruz) as a loading control.

RNA isolation. Total RNA was isolated by Trizol (Invitrogen). Extraction was carried out according to the manufacturer's instructions.

Quantification of miRNAs with real-time PCR. We used TaqMan MiRNA assays to quantify mature miRNAs as described previously[24]. Each reverse transcriptase (RT) reaction contained 10 ng of purified and DNase-treated (Turbo DNA-free, Ambion) total RNA, 50 nM stem-loop RT primer, $1 \times$ RT buffer, dNTPs (each at 1 mM), 16.5 units of MultiScribe Reverse Transcriptase and 1.36 units of RNase inhibitor (Applied Biosystems). The reactions were incubated at 16 °C for 30 min, 42 °C for 30 min and 85 °C for 5 min. Real-time PCR reactions for each miRNA (10 μl volume) were done in triplicate, and each 10 μl reaction mixture included 2 μl of diluted RT product (1:15 dilution), 5 μl of TaqMan 2× Universal PCR Master Mix, 1× TaqMan MiRNA Assay (Applied Biosystems). Reactions were incubated in an Applied Biosystems 7900HT Fast Real-Time PCR system in 384-well plates at 95 °C for 10 min, followed by 40 cycles at 95 °C for 15 s and 60 °C for 1 min. We used the $2-(\Delta\Delta Ct)$ method[17] to determine relative quantitative levels of individual miRNAs, using GADPH for normalization, and expressed values as the relative difference compared to the relevant controls. The primers used are described online in **Supplementary Table 1.**

Precursor miRNA qPCR. SuperScript III Platinum One-Step RT-qPCR kit (Invitrogen) was used to quantify precursor miRNAs by RT-qPCR[25]. The precursor miRNAs to be tested were selected according to the colorectal miRNAome identified by Cummins *et al.*[26]. The primers used are described online in **Supplementary Table 1.**

miRNA processing efficiency. The changes in miRNA processing efficiency were plotted as 'relative processing' and 'processing fold'. Relative processing was defined as the ratio of mature to precursor miRNA. Processing fold was defined as the ratio of mature to precursor miRNA in transfected cells divided by the ratio of mature to precursor miRNA in empty vector transfected cells[4].

$$\text{Processing fold} = \frac{2^{-(\Delta Ct.miR/\Delta Ct.Pre-miR)\text{Transfected}}}{2^{-(\Delta Ct.miR/\Delta Ct.Pre-miR)\text{EmptyVector}}}$$

Total RNA was extracted from three independent experiments and the results presented are the means of these.

Northern blot. Forty micrograms of total RNA together with Decade Marker (Ambion) were resolved in 15% denaturing polyacrylamide gel containing 7 M urea in 0.5XTBE buffer system and transferred onto Hybond-N+ membrane (Amersham) in 0.5XTBE. Probes were radioactively labeled with 25 μCie [γ-32P] ATP (PerkinElmer) and T4 kinase (Invitrogen), and purified with Nucaway Spin columns (Ambion). Membranes were UV-cross linked (1200 jules), prehybridized in hybridization buffer and hybridized overnight in the same solution at 37 °C containing the radioactively labeled probed previously heated at 95 °C for 2 min. Membranes were washed at low stringency followed by film exposure. Probes used are described online in **Supplementary Table 1.**

RNA interference. *TARBP2-* and *DICER1-*specific small interfering RNAs (siRNA) were designed and synthesized by Qiagen. Two siRNA duplexes that recognized two different sequences were used against the *TARBP2* gene, and likewise for the *DICER1* gene. *TARBP2* and *DICER1* expression was analyzed by qRT-PCR and protein blotting; pre-miRNA and miRNAs were assessed by qRT-PCR, as described above.

Transfections of *TARBP2* and *DICER1*. The wild-type *TARBP2* expression vector (pLPC- *TARBP2* wt) was constructed by cloning the cDNA corresponding to the wild-type gene *TARBP2* into a pLPC vector. The truncated form of TRBP was constructed by cloning the cDNA corresponding to *TARBP2* truncated from Co115 into a pCMV-Tag4B vector, pCMV-Tag4B- *TARBP2*-Mut. The DICER1 expression vector pCMV-Tag4B-*DICER1* was constructed by cloning the cDNA corresponding to the gene *DICER1* into a pCMV-Tag4B vector. Transfection of Co115 cells was done by electroporating 10^7 cells in 0.8 ml PBS with 40 μg of the vector at 250 V and 975 μF. After electroporation, cells were washed with PBS and seeded in fresh medium. Clones expressing wild-type TRBP were selected in complete medium supplemented with 0.5 μg ml⁻¹ puromycin; clones expressing the truncated form of TRBP were selected in complete medium supplemented with 1 mg ml⁻¹ G418; clones expressing DICER1 were selected in complete medium supplemented with 1 mg ml⁻¹ G418 and clones coexpressing TRBP wild-type and DICER1 were selected in complete medium supplemented with 0.5 μg ml⁻¹ puromycin and 1 mg ml⁻¹ G418.

Transfection of miRs precursor molecules. miR-19a, miR-138, miR-30a, miR-148a, miR-12b1, miR-125b2 and miR let7a precursor molecules and negative control miRNAs were purchased from Ambion. We carried out experiments involving transient transfections of pre-miRNAs with oligofectamine (Invitrogen) using 100 nmol/l RNA duplexes. The cells were collected 48 h and 72 h after transfection, and the expression of precursor and mature miRNAs was assessed by qRT-PCR, as described above.

miRNA expression study by microarray. Briefly, 5 μg of RNA from each tissue sample was labeled with biotin by reverse transcription using random octomers. Hybridization was carried out on the second version of a miRNA-chip[18], which contained 238 probes for mature miRNAs. Each oligo was printed in duplicate in two different slide locations. Hybridization signals were detected by biotin binding of a Streptavidin-Alexa647 conjugate (one-color signal) using a GenePix 4000B scanner (Axon Instruments). We quantified images using the GenePix Pro 6.0 (Axon Instruments). Raw data were analyzed in

BRB-ArrayTools developed by R. Simon and A.P. Lam (version: 3.6.1, May 2008; National Cancer Institute). Expression data were normalized by quantiles method of the Bioconductor package. Statistical comparisons were done using class comparison *t*-test.

Cell viability and colony formation assay. We determined cell viability by the 3-(4,5-dimethyl-2-thiazolyl)-2,5-diphenyl-2H-tetrazolium bromide (MTT) assay. For colony formation experiments, stable G418, puromycin and G418+ puromycin-resistant colonies were fixed and stained with MTT reagent.

Mouse xenograft model. Athymic *nu/nu* mice, aged 4–5 weeks, were used for tumor xenografts. The animals were maintained in a sterile environment; their cages, food and bedding were sterilized by autoclaving. The experimental design was approved by the IDIBELL animal facility committee. Mice were anesthetized and tumor cells were subcutaneously injected. We subcutaneously injected 3×10^6 of empty vector cells (control) or cells stably transfected with *TARBP2* wild-type, *TARBP2* truncated form, *DICER1* and *TARBP2* wild-type + *DICER1* diluted in 200 μl of PBS in both flanks of each animal ($n = 10$). Mice were weighed, and tumor width (W) and length (L) were measured every 5 d. Tumor volume was estimated according to the formula $V = \pi/6 \times L \times W^2$. Mice were killed 30 d postinjection, and tumors from both groups were excised and weighed. The mean volume or tumor mass ± s.e.m. were calculated for each mouse group, and significance was assessed by means of a two-tailed independent samples *t*-test.

Accession codes. ArrayExpress: miRNA-chip, A-MEXP-258 and E-MTAB-83.

Note: Supplementary information is available on the Nature Genetics website.

AUTHOR CONTRIBUTIONS
S.A.M., S. Ropero and M.E., study and experimental design; C.M. and A.F.F., genomic sequencing; G.A.C., S. Rossi and C.-G.L., microRNAarray hybridization and statistical analysis; B.F., FISH experiments; A.V., animal experiments. L.A.A., H.Y., F.C., C.O., G.C., S.S. and R.S. provided essential reagents, biological samples and intellectual support; S.A.M. and M.E. wrote the manuscript.

Published online at http://www.nature.com/naturegenetics/
Reprints and permissions information is available online at http://npg.nature.com/reprintsandpermissions/

1. Lu, J. *et al.* MicroRNA expression profiles classify human cancers. *Nature* **435**, 834–838 (2005).
2. Calin, G.A. & Croce, C.M. MicroRNA signatures in human cancers. *Nat. Rev. Cancer* **6**, 857–866 (2006).
3. Gaur, A. *et al.* Characterization of microRNA expression levels and their biological correlates in human cancer cell lines. *Cancer Res.* **67**, 2456–2468 (2007).
4. Thomson, J.M. *et al.* Extensive post-transcriptional regulation of microRNAs and its implications for cancer. *Genes Dev.* **20**, 2202–2207 (2006).
5. Saito, Y. *et al.* Specific activation of microRNA-127 with downregulation of the proto-oncogene BCL6 by chromatin-modifying drugs in human cancer cells. *Cancer Cell* **9**, 435–443 (2006).
6. Lujambio, A. *et al.* Genetic unmasking of an epigenetically silenced microRNA in human cancer cells. *Cancer Res.* **67**, 1424–1429 (2007).
7. Lujambio, A. *et al.* A microRNA DNA methylation signature for human cancer metastasis. *Proc. Natl. Acad. Sci. USA* **105**, 13556–13561 (2008).
8. Chang, T.C. *et al.* Widespread microRNA repression by Myc contributes to tumorigenesis. *Nat. Genet.* **40**, 43–50 (2008).
9. Kumar, M.S., Lu, J., Mercer, K.L., Golub, T.R. & Jacks, T. Impaired microRNA processing enhances cellular transformation and tumorigenesis. *Nat. Genet.* **39**, 673–677 (2007).
10. Chendrimada, T.P. *et al.* TRBP recruits the Dicer complex to Ago2 for microRNA processing and gene silencing. *Nature* **436**, 740–744 (2005).
11. Haase, A.D. *et al.* TRBP, a regulator of cellular PKR and HIV-1 virus expression, interacts with Dicer and functions in RNA silencing. *EMBO Rep.* **6**, 961–967 (2005).
12. Herman, J.G. *et al.* Incidence and functional consequences of hMLH1 promoter hypermethylation in colorectal carcinoma. *Proc. Natl. Acad. Sci. USA* **95**, 6870–6875 (1998).
13. Fleisher, A.S. *et al.* Hypermethylation of the hMLH1 gene promoter in human gastric cancers with microsatellite instability. *Cancer Res.* **59**, 1090–1095 (1999).
14. Lynch, H.T. & de la Chapelle, A. Hereditary colorectal cancer. *N. Engl. J. Med.* **348**, 919–932 (2003).
15. Markowitz, S. *et al.* Inactivation of the type II TGF-beta receptor in colon cancer cells with microsatellite instability. *Science* **268**, 1336–1338 (1995).
16. Rampino, N. *et al.* Somatic frameshift mutations in the BAX gene in colon cancers of the microsatellite mutator phenotype. *Science* **275**, 967–969 (1997).
17. Livak, K.J. & Schmittgen, T.D. Analysis of relative gene expression data using real-time quantitative PCR and the 2(-Delta Delta C(T)) Method. *Methods* **25**, 402–408 (2001).
18. Calin, G.A. *et al.* Ultraconserved regions encoding ncRNAs are altered in human leukemias and carcinomas. *Cancer Cell* **12**, 215–229 (2007).
19. Hammond, S.M. MicroRNAs as tumor suppressors. *Nat. Genet.* **39**, 582–583 (2007).
20. Gregory, P.A. *et al.* The miR-200 family and miR-205 regulate epithelial to mesenchymal transition by targeting ZEB1 and SIP1. *Nat. Cell Biol.* **10**, 593–601 (2008).
21. Sander, S. *et al.* MYC stimulates EZH2 expression by repression of its negative regulator miR-26a. *Blood* **112**, 4202–4212 (2008).
22. Scott, G.K. *et al.* Coordinate suppression of ERBB2 and ERBB3 by enforced expression of micro-RNA miR-125a or miR-125b. *J. Biol. Chem.* **282**, 1479–1486 (2007).
23. Karube, Y. *et al.* Reduced expression of Dicer associated with poor prognosis in lung cancer patients. *Cancer Sci.* **96**, 111–115 (2005).
24. Raymond, C.K., Roberts, B.S., Garrett-Engele, P., Lim, L.P. & Johnson, J.M. Simple, quantitative primer-extension PCR assay for direct monitoring of microRNAs and short-interfering RNAs. *RNA* **11**, 1737–1744 (2005).
25. Schmittgen, T.D., Jiang, J., Liu, Q. & Yang, L. A high-throughput method to monitor the expression of microRNA precursors. *Nucleic Acids Res.* **32**, e43 (2004).
26. Cummins, J.M. *et al.* The colorectal microRNAome. *Proc. Natl. Acad. Sci. USA* **103**, 3687–3692 (2006).